5.2 DESCRIPTION AND EVALUATION OF THE QUIC DROPLET SPRAY SCHEME: DROPLET EVAPORATION AND SURFACE DEPOSITION

Dragan Zajic*, Matthew A. Nelson, Michael D. Williams, and Michael J. Brown
Los Alamos National Laboratory, Los Alamos, NM

1. Introduction

The Quick Urban and Industrial Complex (QUIC) dispersion modeling system was developed with the goal of improving the transport and dispersion modeling capabilities within urban areas. The modeling system has the ability to rapidly obtain a detailed 3D flow field around building clusters and uses an urbanized Lagrangian random-walk approach to account for transport and dispersion (e.g., see Singh et al., 2008; Williams et al., 2009; and Gowardhan et al., 2009). In addition to wind-tunnel testing, the dispersion modeling system has been evaluated against full-scale urban tracer experiments performed in Salt Lake City, Oklahoma City, and New York City (Gowardhan et al., 2006; Gowardhan et al., 2009; Allwine et al., 2008) and the wind model output to measurements taken in downtown Oklahoma City (see this conference Neophytou et al., 2010).

Several dispersion models (e.g., SCIPUFF, VLSTRACK, AgDRIFT) contain spray droplet source terms for counter-terrorism and/or agricultural pesticide applications (Sykes et al., 2008; Bauer and Gibbs, 1998; Teske et al., 2002). In this paper, we provide a description of the gravitational settling, droplet evaporation and deposition schemes that make up the QUIC wet slurry scheme. We evaluate the droplet evaporation algorithms as a function of temperature and relative humidity by comparing the predicted droplet size as a function of time to other theoretical models by Kukkonen (1989), Morawska (2006) and Hinds (1999, 2001) as well as to experimental measurements by Houghton (1933). The paper ends with a description of outdoor droplet spray experiments performed by Fritz and Hoffman (2008) and a comparison between the deposition measurements and the QUIC-computed deposition fields.

*Corresponding author address: Dragan Zajic, LANL, Group D-3, MS K575, Los Alamos, NM 87545, dzajic@lanl.gov.

Release number: LA-UR-10-00204.

2. The QUIC Wet-Slurry Scheme

The wet-slurry option available within the QUIC dispersion modeling system enables calculations of the dispersion of non-soluble particles suspended in water after they are emitted as a droplet spray. The user specifies the initial droplet size distribution, the amount of active non-soluble particles, the concentration of non-active inert solids in the solution, the effective density of the dry agglomerate, the relative humidity and temperature of the air, and the atmospheric pressure. The droplets will evaporate with time as they move through the air while simultaneously being pulled downwards by gravity. The settling velocity of each droplet will change with time as its radius decreases due to evaporation. Droplets that reach the ground or building walls will settle out and deposit some of their mass to the surface. If the droplet completely evaporates before reaching the ground, a dry agglomerated particle made up of active particles and inert solids will remain and be tracked. The size of the dry particle is determined by the initial concentration of solids in the solution and by the effective density of the dry agglomerate. The former determines the solids mass in each droplet and the latter provides an estimate of how tightly packed the solids are when dry.

2.1 Gravitational Settling Scheme

The gravitational settling velocity for an aerosol particle is based on Stokes' Law for the terminal velocity of spherical particles with a slip correction factor for small diameter (d_p) particles. The terminal velocity (v_s) is calculated using (e.g., Finlayson-Pitts, 1986; Seinfeld and Pandis, 1998):

$$v_s = \frac{1}{18}\frac{d_p^2 \rho_p g}{\mu_{air}} C_C \qquad (1)$$

where ρ_p is the particle density, g is gravitational acceleration, μ_{air} is the absolute viscosity of air, and C_C is the so-called Cunningham's correction factor.

The correction factor is approximated by:

$$C_C = 1 + \frac{2\lambda}{d_p}\left[1.257 + 0.4\exp\left(-\frac{1.1 d_p}{2\lambda}\right)\right] \quad (2)$$

where λ is the mean free path of air. Seinfeld and Pandis (1998) show that the correction factor becomes more important for small particles, for example, C_C = 22.2, 2.85, 1.164, and 1.016 for d_p = 0.01, 0.1, 1 and 10 μm, respectively, at standard temperature and pressure.

The characteristic time scale to reach terminal velocity is very small, e.g., $3x10^{-4}$, $4x10^{-6}$, and $9x10^{-8}$ s for d_p = 0.1, 1 and 10 μm, respectively, so that use of the terminal velocity is a good approximation for the particle fall velocity. Note that we do not account for shape deformation of the water droplet.

2.2 Evaporation Scheme

Within the wet-slurry option, the evaporation algorithm is enacted for marker particles (i.e., water droplets) having a radius larger than the final dry agglomerate particle radius (Williams et al., 2009). The time rate of change of the droplet radius *r* [m] due to evaporation is computed using (e.g., see Seinfeld and Pandis, 1998):

$$\frac{dr}{dt} = \frac{D_{corr}\left(101325\left(P_v - P_d\right)\right)}{10^6 \rho r\left(\frac{D_{corr} H_v 101325 P_d\left(\frac{H_v}{RT} - 1\right)}{M_v k_{corr} T} + \frac{RT}{M_v}\right)} \quad (3)$$

where *dr/dt* is the time rate of change of the droplet radius [m/s], D_{corr} is the corrected diffusion coefficient of water vapor in air [m^2/s], P_v is the ambient water vapor pressure of the atmosphere [atm], P_d is the vapor pressure of water at the surface of the droplet [atm] (the factor of 101,325 converts both vapor pressures into Pascals), ρ is the density of liquid water [g/mL] (the factor of $1x10^6$ converts the density to g/m^3), H_v is the heat of vaporization of water [J/mol], *R* is the universal gas constant [8.314151 J/(molK)], *T* is the local atmospheric temperature [K], M_v is the molecular weight of water agent vapor [g/mol] and k_{corr} is the corrected thermal conductivity of air [W/(mK)]. Below we show how each of these terms is computed.

To obtain D_{corr}, the molecular diffusion coefficient *D* [m^2/s] is first computed based on Hall and Pruppacher (1976) and Pruppacher and Klett (1978):

$$D = 2.11 \cdot 10^{-5}\left(\frac{T}{T_0}\right)^{1.94}\left(\frac{P_0}{P}\right) \quad (4)$$

where T_0 is the reference air temperature [273.15 K], P_0 is the reference pressure [1 atm], *T* is the local air temperature [K], and *P* is the local pressure [atm]. The diffusion coefficient is then corrected for non-continuum effects through ventilation and collision geometry terms:

$$D_{corr} = D\frac{C_{vent}}{C_{coll}}. \quad (5)$$

As determined by Beard and Pruppacher (1971), the ventilation coefficient C_{vent} is a function of the Reynolds number (*Re* = *Ud/v*) and the Schmidt number (*Sc* = *v* /*D*), where *U* is the droplet speed [m/s], *d* is the particle diameter [m], and *v* is the kinematic viscosity of air [m^2/s]:

$$C_{vent} = 1 + 0.108\,\mathrm{Re}\,Sc^{2/3} \qquad \text{for } \mathrm{Re}^{1/2}Sc^{1/3} \le 1.4$$
$$C_{vent} = 0.78 + 0.308\,\mathrm{Re}^{1/2}\,Sc^{1/3} \qquad \text{for } \mathrm{Re}^{1/2}Sc^{1/3} > 1.4 \quad (6)$$

The collision coefficient C_{coll} is a function of a geometry coefficient and a sticking coefficient:

$$C_{coll} = 1 + (C_{geom} + C_{stick})\frac{MFP}{r} \quad (7)$$

where

$$C_{geom} = 1.33 + \frac{0.70\, r/MFP}{1 + r/MFP} \quad (8)$$

and

$$C_{stick} = \frac{4 \cdot (1 - E_{stick})}{3E_{stick}}. \quad (9)$$

Here, *r* is the radius of the droplet [m], *MFP* is the mean free path of water in the vapor phase [m], and E_{stick} is the sticking efficiency (between 0 and 1). For water vapor, the sticking efficiency is set to one (Prupacher and Klett, 1978).

The vapor pressure P_v of the ambient atmosphere is determined from the relative humidity profile and the saturation vapor pressure of water:

$$P_v(z) = rh(z) * P_{sat}. \quad (10)$$

The saturation vapor pressure P_{sat} [atm] is computed using (Jacobson 2005):

$$P_{sat} = P_{sat0} \exp\left(\frac{M_v}{R} \left(A \left(\frac{T - T_0}{T T_0} \right) + B \ln\left(\frac{T}{T_0} \right) \right) \right) \quad (11)$$

where P_{sat0} is the reference vapor pressure of water [6.03x10^{-3} atm], M_v is the molecular weight of water vapor [g/mol], R is the universal gas constant [8.314151 J/(molK)], T is the atmospheric temperature as function of height [K], T_0 is the reference temperature [273.15 K], A has a value of 3.14839 x 10^3 J/g, and B has a value of 2.370 J/(gK).

The vapor pressure of water at the surface of the droplet P_d [atm] is:

$$P_d = P_{sat} \exp\left[\frac{2\sigma M_{liq}}{rRT(1x10^6 \rho_{liq})} \right] \quad (12)$$

where σ is the surface tension of the water droplet [N/m], M_{liq} is the molecular weight of liquid water [g/mol], r is the radius of the droplet [m], and ρ_{liq} is the liquid density of water [g/mL] (the factor of 1x10^6 converts the density to g/m^3). The water droplet surface tension is calculated using:

$$\sigma = 0.001 \cdot (76.1 - 1.55(T - T_0)) \quad \text{if T} \geq \text{T}_0$$
$$\sigma = \sum_{i=1}^{7} \alpha_i (T - T_0)^i \quad \text{if T} < \text{T}_0 \quad (13)$$

where α_1 = 7.593 x 10^{-2}, α_2 = 1.15 x 10^{-4}, α_3 = 6.818 x 10^{-5}, α_4 = 6.511 x 10^{-6}, α_5= 2.933 x 10^{-7}, α_6 = 6.283 x 10^{-9}, and α_7 = 5.285 x 10^{-11}.

The heat of vaporization H_v [J/mol] is determined from:

$$H_v = (2501 - 2.37 \cdot (T - T_0)) \cdot M_{liq} \quad (14)$$

while the corrected thermal conductivity of air k_{corr} [W/(mK)] is specified using:

$$k_{corr} = k \frac{C_{vent}}{C_{coll}} \quad (15)$$

where C_{vent} and C_{coll} are as defined above with the exception of the Schmidt number, the mean free path of the agent vapor, and the sticking efficiency being replaced with the Prandtl number $Pr = \rho v C_p / k$ (where C_p is the heat capacity of air [J/(kgK)]), the mean free path of air, and the thermal accommodation of air, respectively.

2.3 Deposition Scheme

Deposition of gases and aerosols is computed internally in the QUIC random-walk code if the deposition velocity scheme is turned on. We do not use a sticking factor approach, i.e., where some fraction of the marker particles that impact surfaces stick to the surface and are then removed from the transport and dispersion simulation calculation. Rather, when marker particles are close to surfaces (within one grid cell) a fraction of the particle mass (f_{dep}) is lost to the surface using the traditional deposition velocity (v_d) approach:

$$f_{dep} = 1 - \exp\left(-\frac{v_d \cdot \Delta t}{\Delta z_b} \right). \quad (16)$$

Here Δt is the random-walk time step and Δz_b represents the depth of the concentration grid cell normal to a surface. As described in more detail in Williams et al. (2009) this equation is derived by setting the time rate of change of mass in a grid cell adjacent to a surface equal to the deposition rate at the surface and integrating over the time step Δt. This integration was done to ensure mass conservation over the time step, as a constant concentration assumption over a time step is invalid for large particles with large gravitational settling velocities.

The mass deposited to the surface by the marker particle in one time step is:

$$M_{Dep} = m_p(t) \cdot \left\{ 1 - \exp\left(-\frac{v_d \cdot \Delta t}{\Delta z_b} \right) \right\}. \quad (17)$$

The total mass deposited is determined by summing over all particles in the collecting box of interest and summing over time.

A resistance-based approach is used to compute the deposition velocity (e.g., see Seinfeld and Pandis, 1998):

$$v_d = \frac{1}{r_a + r_b + r_a r_b v_s} + v_s \quad (18)$$

where r_a is the aerodynamic resistance, r_b is the quasi-laminar surface resistance, and v_s is the gravitational settling velocity. Note that v_s is set to zero for vertical surfaces (e.g., walls) and for gases. Note also that the form of the equation above assumes that the surface or canopy resistance r_c =

0, a valid assumption for aerosol particles, but not for gases. The aerodynamic resistance r_a is the parameter that accounts for the impact of the turbulent atmosphere in transporting material from the air to a ground surface. In higher turbulence intensity environments dry deposition is enhanced, while for low turbulence intensities dry deposition is reduced. QUIC uses the formula proposed by Sehmel and Hodgson (1978):

$$r_a = \frac{1}{\kappa u_*} \ln\left[\frac{\frac{10{,}000 u_* \Delta z_b}{2\nu} + \frac{1}{Sc}}{\frac{100 u_*}{\nu} + \frac{1}{Sc}} \right], \qquad (19)$$

where ν is the kinematic viscosity of air, $Sc = \nu/D$ is the Schmidt number, and D is mass diffusivity. The quasi-laminar or surface resistance r_b represents the viscous layer(s) near surfaces through which the airborne contaminant must pass to get to the surface. For gases and small particles (St <10)

$$r_b = \frac{1}{u_* Sc^{-2/3}} \qquad (20)$$

For large particles (St > 10)

$$r_b = \frac{1}{u_* \left(Sc^{-2/3} + 10^{-3/St} \right)} \qquad (21)$$

where $St = v_s u_*^2 / g\nu$ is the Stokes number.

3. Evaluation of the Evaporation Scheme

Houghton (1933) performed experiments on the evaporation of fog droplets inside of an enclosed chamber with negligible air currents (<2 cm/s). The droplets were suspended from fine wires or glass filaments in the chamber and the diameter was measured as a function of time using an ocular micrometer in a low power microscope. The humidity and temperature inside the chamber were kept constant during each experiment. The range of initial droplet sizes during the experiment was between 25 and 2600 microns and readings were taken at 30 second to ten minute intervals depending on the rate of evaporation. The cases presented here show evaporation of droplets of initial size of approximately 500 microns and between 900 and 1000 microns at different temperatures and relative humidity (see Figs. 1 and 2).

Since the droplets were not falling in the experiment, the ventilation term in the QUIC evaporation algorithm was turned off. We have also included curves that show model output with the ventilation term turned on just to illustrate the impact of the terminal fall velocity on the evaporation rate; however, these should not be considered when judging the performance of the model. Figure 1 shows three experiments for water droplets with an initial size of between 900 and 1000 microns. Two of the cases have 0% relative humidity, but one was conducted in cold air (4.8 °C) and the other in warm air (22 °C). The third case was performed in warm air (20.3 °C) and higher relative humidity (42%). As expected the droplets evaporated more quickly for the warm dry air case, while the droplets took slightly longer to evaporate for the cold dry air case as compared to the warm, moderately wet air case. In all 3 cases, the QUIC evaporation scheme slightly under estimated the droplet evaporation rate with droplet drying times typically over estimated by less than 10%.

Figure 2 shows comparisons of experimental results and QUIC calculations for warm air cases over a range of relative humidity (0%, 53%, 88%) for initial droplet diameters of roughly 500 microns. The QUIC calculations for zero ventilation compare reasonably well for the dry air case, slightly overestimate the evaporation rate for rh = 53% (drying time underestimated by ~20%), and underestimate the evaporation rate for rh = 88% (drying time overestimated by ~37%).

The degraded performance for higher relative humidity is troubling. However, when compared to other evaporation models by Kukkonen et al. (1989), Morawska (2006), and Hinds (1999, 2001) for falling water droplets, i.e., ventilation turned on, the QUIC model performed reasonably well. Figure 3 depicts the QUIC-computed droplet diameter versus time compared to the Kukkonen et al. (1989) and Morawska models over a range of relative humidity. For relative humidity in the range from 0 to 60%, the QUIC evaporation scheme results are in a very good agreement with calculations of the other two models. For rh = 80%, the QUIC evaporation is actually slightly faster as compared to the Morawska model.

The model of Kukkonen et al. (1989) numerically solves equations of mass and heat transfer from a droplet surface including forced convection of mass and heat due to free fall. Their evaporation studies of freely falling droplets of water were performed at a gas temperature of 20°C while the vapor pressure in the gas was reported as negligible, i.e., low relative humidity. Morawska's calculations of 100 micron droplet evaporation were conducted for different relative humidity with an air temperature of 25°C.

Predicted droplet drying times for the Hinds (1999, 2001) model are compared to the QUIC model in Figure 4. The drying time calculations were performed for different initial water droplet sizes at a temperature of 20 °C in dry and humid air. For relative humidity of 0 and 50% there is very good agreement between the QUIC results and Hinds' calculations. For a relative humidity of 100%, the QUIC drying times are longer than Hinds' calculations by up to a factor of 2. The details of the evaporation model are given in Hinds (1999). We are currently investigating the differences between the models to understand the differences. One such difference is that the Hinds model for computing the partial pressure on the droplet surface is obtained using a Kelvin equation that accounts for the surface curvature of the droplet.

4. Evaluation of Deposited Mass from an Aerial Sprayer

4.1 Experimental Description

The results of deposition measurements from the aerial spraying field experiment conducted by Fritz and Hoffmann (2007) were used to evaluate the QUIC droplet spray scheme. During this study an AirTractor AT-402B plane with spray boom was used to disseminate droplets consisting of water, Trition X-100 surfactant at 0.1% v/v, and Caracid Brilliant Flavine FFN fluorescent dye at 15 g/ha. The swath width was 20 m and the height of application was 2.4 m above ground level. The spray boom nozzles produced droplets of volume median diameter (VMD) of 236 microns. The complete initial droplet size distribution was not given, but they did report that the percentage of spray volume contained in droplets less than 200 microns was 34% and the percentage of spray volume in droplets less than 100 microns was 14%. The direction of the flight line was normal to the wind (see Fig. 5) and downwind sampling locations were located in the center of a large (approx. 70 ha) square flat field of wheat stubble 10 to 20 cm tall. Three sub-samples of mylar collectors at multiple downwind distances were used to measure spray deposition. Monofilament nylon screen cylinders positioned at multiple heights (0.3, 3, and 6 m) and downwind distances on sampling towers collected the airborne portion of the spray (Fig. 5).

Wind speed, wind direction, temperature and humidity were measured on a tower 100 m downwind of the flight line at 2.5, 5 and 10 meters above the ground. These measurements enabled calculations of atmospheric thermal stability via the gradient Richardson number Ri. The tower instruments measured one-minute averages of wind speed and direction (RM Young model 05701 Wind Monitor-RE) and temperature (RM Young model 43347VC Temperature Probes). Relative humidity was measured with an RM Young model 71372 temperature/relative humidity sensor. Table 1 provides information on atmospheric conditions during each of the performed tests. Tables 2 and 3 give the deposition measurement results as a percentage of applied material reported by Fritz and Hoffmann (2007).

4.2 QUIC Set-up

The QUIC simulation input was set to closely match the meteorological and spraying conditions during the selected field tests. For this paper, two cases were selected: one with high humidity (Rep 2) and the other with lower humidity (Rep 9). Rep 9 was conducted at 7:36 PM, the atmospheric temperature was 33.5°C, the relative humidity was 42% and the wind speed at 2.5 m above ground level was 1.9 m/s. The gradient Richardson number calculated from the measured wind speed and temperature was 0.081. Since the stability conditions in QUIC modeling system are set using the inverse Monin-Obukhov scale 1/L, the Ri value reported was converted to 1/L using the expression (Neumann 1961):

$$Ri = \frac{z}{L}\left(1 + \beta \frac{z}{L}\right). \qquad (22)$$

where $\beta = -0.6$. The calculated value of 1/L for Rep 9 is 0.047 m^{-1} which approximately corresponds to Pasquill's stability class E (Golder 1972, Arya 1999) for a roughness length between 1 and 2 cm (about 10% of the reported wheat stubble height).

Rep 2 was conducted in the morning at 7:43AM when the temperature was 23°C, the relative humidity was 92.1%, and the wind speed was only 0.4 m/s. The gradient Richardson number value of -0.77 indicates unstable thermal conditions and converts to 1/L=-0.24 m^{-1} which belongs to Pasquill stability class A. An A stability class at this time in the morning seems unlikely, so we also performed a QUIC calculation for neutral thermal stability.

QUIC uses lognormal functions to define the initial droplet size distribution. In order to better represent the distribution of the smaller droplets, the QUIC setup used a lognormal size distribution by numbers with count median diameter (CMD) set to

50 microns (VMD was 220 micron) and a standard deviation (SD) of 2.1. For these values, 54.6% of the volume is carried by droplets of size smaller than 236 microns, while the volume fraction carried by droplets smaller than 100 and 200 microns is 12.1% and 44.4%, respectively. As compared to the reported values (50% of volume less than 236 microns, 34% < 200 microns, and 14% < 100 microns), we are slightly underestimating the volume of droplets below 100 microns.

The QUIC source definition module does not have the ability to account for vortices created by the wings of the airplane. As indicated by Teske et al. (2002), the wing-induced vortices can loft the spray droplets up into the air resulting in different patterns of near source deposition, especially for low-flying aircraft. The vortices remain for some time before they die out. Although not entirely satisfactory, our preliminary approach to approximate the effects of the vortices was to define the source as a rectangular box (see Fig. 6). Three box sizes were tested. The base case is an elevated rectangular volume source of size 600 m long x 20 m wide (i.e., flight path length x boom width) x 0.1 m deep located 2.35 m above the ground (green dashed line in Fig. 7). The second case has the same length and width as the base case, but is 2.4 m deep and extends from the boom height to the ground (red line). The third source geometry expands the source height vertically and laterally by assuming that radius of the largest vortex is the distance between the ground and the wing resulting in a box 4.8 m deep and 24.8 m wide (blue dashed line).

Deposition was calculated by QUIC on a horizontal uniform grid of size 10 m x 10 m and then summed up for different areas of interest in order to compare to the measurements reported in the tables: in-swath (-20-0 m just under source), 0-10m, 10-20m, 20-30m, 30-40m, 40-50m, 50-75m, 75-100m, 100-150m, and 150-200m down-wind of the spray location. Note that in the deposition plots shown in the next section, the in-swath deposition occurs at x=0, while is centered at the corresponding area where deposition is calculated. The regions spans laterally across the whole domain and each calculated deposited mass is normalized by the mass of released spray

5. Deposition results

Figures 7 and 8 show comparisons of the experimental measurements and QUIC modeling results of deposition vs. downwind distance for Rep 9 and 2, respectively. For the evening case with light winds, stable atmospheric conditions, and 42% relatively humidity (Rep. 9), the in-swath calculated deposition masses are about double the measured values (Fig. 7). The QUIC model indicates that nearly 80% of the droplets have fallen out immediately below the in-swath spray zone as compared to roughly 40% as shown by the measurements. Minimal differences are seen between the four different QUIC simulations, indicating that the initial box size and atmospheric stability are not important factors for the in-swath deposition. As expected, since the QUIC model overestimates deposition near the source, the model underestimates deposition downwind. In this region, the best performing modeling results are for the case when the source is represented as a thin rectangular box placed at boom height (denoted as QUIC 4) and values are about the half of the measured values. The worst performance is for the neutral stability run (QUIC 1) where the values are at least 4 times lower than field test results.

Figure 8 shows the comparisons for Rep. 2, which was characterized by higher humidity, light winds, and unstable atmospheric stability. For this case, the computed in-swath deposition for all the QUIC runs (74-94%) is close to the measured value (78%), especially for the neutral case (QUIC 1). QUIC deposition values again drop rapidly with downwind distance and are significantly lower than measured. In this case the modeled downwind deposition values are about an order of magnitude lower than measured.

For both cases, the reason for the underestimation of deposited mass further downwind could be multiple. First, the actual initial droplet size distribution is not well known, especially for the smaller droplets. If we have underestimated the number of droplets in the smaller size bins (e.g., 10-50 microns), we will likely underestimate the downwind deposition as these are the sizes most likely to not fallout in-swath and survive further downwind. The second reason is due to not including the flow field resulting from the wing-induced vortices which would increase the upward momentum of sprayed droplets and contribute to their downwind transport. In spite of this, the model results were within a factor of two for the lower humidity case (Rep. 9). For the higher humidity case (Rep. 2), the reason for the larger discrepancy in downwind deposition could be due to the underestimated evaporation rate at high humidity that we found in Section 3. The slower evaporation means the drops reduce their size more slowly and thus fall to the ground sooner due to their larger

terminal velocity, ultimately reducing the deposition further downwind.

We suspect that the overestimation of the droplet deposition near the source for Rep. 9 is due to QUIC not accounting for the velocity field created by the wing-induced vortices. As described by (Trayford and Welch 1977), even large 500 micron droplets can be swept upwards by these vortices, thereby reducing the deposited fraction in-swath. In light of the discussion above, the good in-swath results for Rep. 2 are difficult to understand, however. In theory, the QUIC model should overestimate the in-swath deposition due to 1) the lack of wing-induced vortices and 2) underestimating the evaporation rate at high relative humidity.

6. Conclusions

The spray droplet scheme in QUIC has been described, including the equations for droplet evaporation, gravitational settling, and deposition. The evaporation rate plays an important role in the dispersal and deposition pattern of droplet spray releases. The evaporation scheme implemented within the QUIC compared well with water droplet evaporation experiments at low and intermediate relative humidity (rh), but at higher rh QUIC underestimated the evaporation rate of droplets.

QUIC was then tested against a wet slurry release from an airplane. Model-computed deposition was within a factor of two for the case with rh=42% with overestimation within the in-swath region and underestimation in the downwind area. For the case with higher rh, the model-computed deposition in-swath was in reasonable agreement with the measurements, but performance downwind degraded with the model underestimating deposition by about an order of magnitude.

In the future, we intend to investigate why the evaporation scheme does not work as well at high humidity and will compare the performance of different schemes found in the literature. We will expand our model evaluation assessments to include evaporation of falling droplets. We may try to incorporate the momentum of wing-induced vortices into our near-source droplet release model (similar to AgDrift) in order to better capture the in-swath and downwind deposition patterns from low-level fixed wing releases.

7. References

Allwine K.J., Flaherty J.E., Brown M., Coirier W., Hansen O., Huber A., Leach M., and Patnaik G., 2008: Urban Dispersion Program: Evaluation of six building-resolved urban dispersion models, Official Use Only PNNL-17321 report, 88 pp.

Arya S.P., 1999: *Air Pollution Meteorology and Dispersion*, Oxford University Press, 310 pp.

Bauer, T.J. and R.L.Gibbs, 1998: Software user's manual for the Chemical/Biological Agent Vapor, Liquid, and Solid Tracking (VLSTRACK) computer model, version 3.0. NSWC Doc. NSWCDD/TR-98/62, Systems Research and Technology Department, Dahlgren Division, Naval Surface Warfare Center, Dahlgren, VA, 170pp.

Beard, K. V. and H. R. Pruppacher, 1971: A wind tunnel investigation of the rate of evaporation of small water drops falling at terminal velocity in air, J. Atmos. Sci., 28, 1455-1464.

Finlayson-Pitts B.J. and Pitts J.N. Jr., 1986: Atmospheric chemistry. Fundamentals and experimental techniques, John Wiley and Sons, New York, NY, 1125 pp.

Fritz B.K and Hoffmann W.C, 2007: Meteorological Influences on Mass Accountability of Aerially Applied Sprays, 2007 ASABE/NAAA Technical Session, 41st Annual National Agricultural Aviation Association Convention, Silver Legacy Resort, Reno, Nevada, December 10, 2007.

Golder D., 1972: Relations among stability parameters in the surface layer, *Boundary-Layer Meteorology* 3: 47-58.

Gowardhan A., Brown M. J., Pardyjak E. R., Williams M. D. and Nelson M. A., 2009: Evaluation of the QUIC wind and dispersion models using the Joint Urban 2003 Field Experiment., *8th Symposium on the Urban Environment, American Meteorological Society, Phoenix, AZ*.

Gowardhan A., Brown M., Pardyjak E.R., 2009: Evaluation of a fast response pressure solver for flow around an isolated cube, *J. Env. Fluid Mech.,* published online, to appear shortly in print.

Gowardhan, A., M. Brown, M. Williams, E. Pardyjak, 2006: Evaluation of the QUIC Urban Dispersion Model using the Salt Lake City URBAN 2000 Tracer

Experiment Data- IOP 10. *6th AMS Symp. Urban Env., Atlanta, GA, LA-UR-05-9017, 13 pp*.

Hall W.D. and Pruppacher H.R 1976, The survival of ice particles falling from cirrus clouds in subsaturated air, *J. Atmos. Sci*., 33: 1995-2000.

Hinds W.C., 1999: *Aerosol Technology*, 2nd Ed. New York: John Wiley & Sons.
Hinds W.C., 2001: Physical and Chemical Changes in the Particulate Phase from *Aerosol Measurements: Principles, Techniques, and Applications*, Second Edition, Edited by Paul A. Baron and Klaus Willeke.

Houghton H.G., 1933: A Study of the Evaporation of Small Water Drops, *Physics*, 4: 419-424.

Jacobson M.Z., 2005: *Fundamentals of Atmospheric Modeling*, Cabridge University Press, 813 pp.

Morawska L., 2006: Droplet fate in indoor environments, or can we prevent the spread of infection?, *Indoor Air*, 16: 335–347.

Kukkonen J., Vesala T. and Kulmala M., 1989: The Interdependence of Evaporation and Settling for Airborne Freely Falling Droplets, *J. Aerosol Sci*., 20: 749-763.

Neophytou M. 2010: An inter-comparison of three urban wind models with Oklahoma City Joint Urban 2003 Experiment wind measurements, *16th Conference on Air Pollution Meteorology, American Meteorological Society, Atlanta, GA*.

Neumann J., 1961: Richardson's number and the Monin-Obukhov wind profile, *Journal of Meteorology*, 18: 808-809.

Pruppacher, H.R. and J.D. Klett, 1978: *Microphysics of Clouds and Precipitation*, D. Reidel Publishing Co., Dordrecht, Holland.

Sehmel G.A. and Hodgson W.H. 1978: Model for predicting dry deposition of particles and gases to environmental surfaces, *AIChE symposium, Philadelphia, PA, USA*.

Seinfeld, J.H. and S.N. Pandis, 1998: *Atmospheric Chemisty and Physics: From Air Pollution to Climate Change* Wiley Interscience, New York, NY, 1326 pp.

Singh, B., B. Hansen, M. Brown, E. Pardyjak, 2008: Evaluation of the QUIC-URB fast response urban wind model for a cubical building array and wide building street canyon, *Env. Fluid Mech*., 8: 281-312.

Sykes, R.I., S.F. Parker, D.S. Henn, and B. Chowdhury, 2008: SCIPUFF Version 2.4 Technical Documentation, 361 pp.

Teske M.E., Bird S.L., Esterly D.M., Curbishley T.B., Ray S.L., Perry S.G., 2002: AgDRIFT: a model for estimating near-field spray drift from aerial applications. Environmental Toxicology and Chemistry, 21(3), 659–671.

Trayford R.S. and Welch L.W., 1977: Aerial Spraying: A Simulation of Factors Influencing the Distribution and Recovery of Liquid Droplets, *J. Agric. Engng Res.* 22: 183-196.

Williams M.D., Brown M.J. and Nelson M.A, 2009: QUIC-PLUME Theory Guide
(Version 5.5).

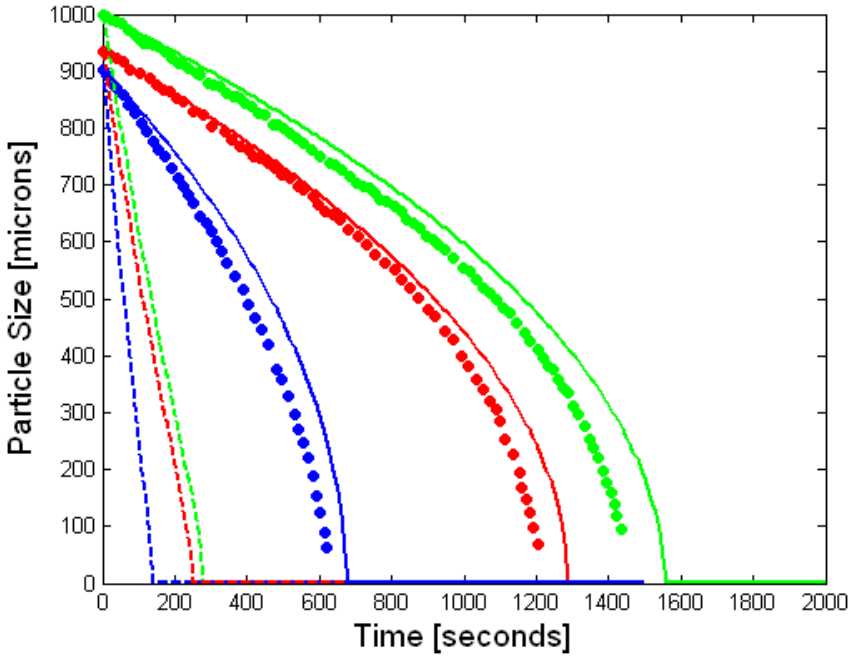

Figure 1. Comparison of stationary droplet evaporation measurements with QUIC calculations (green RH=0% T=4.8C, red RH=42% T=20.3C, blue RH=0% T=22C): experimental measurements (dots), QUIC results with ventilation turned off (solid lines), and QUIC results with ventilation turned on (dashed lines). Note that the experiments correspond most closely to the no ventilation case.

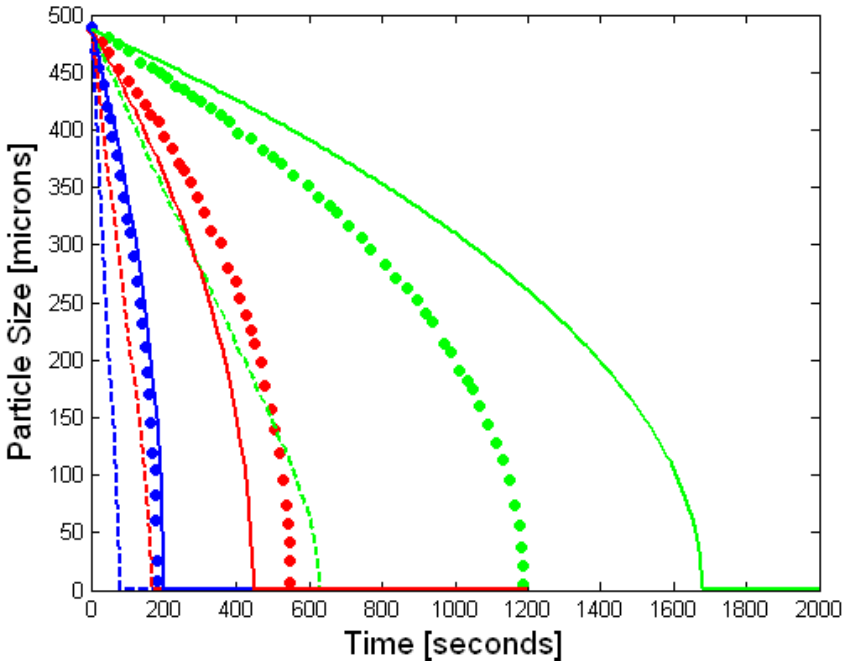

Figure 2. Comparison of stationary droplet evaporation measurements with QUIC calculations (green RH=88% T=20.8C, red RH=53% T=19.6C, blue RH=0% T=21.7C): experimental measurements (dots), QUIC results with ventilation turned off (solid lines), and QUIC results with ventilation turned on (dashed lines). Note that the experiments correspond most closely to the no ventilation case.

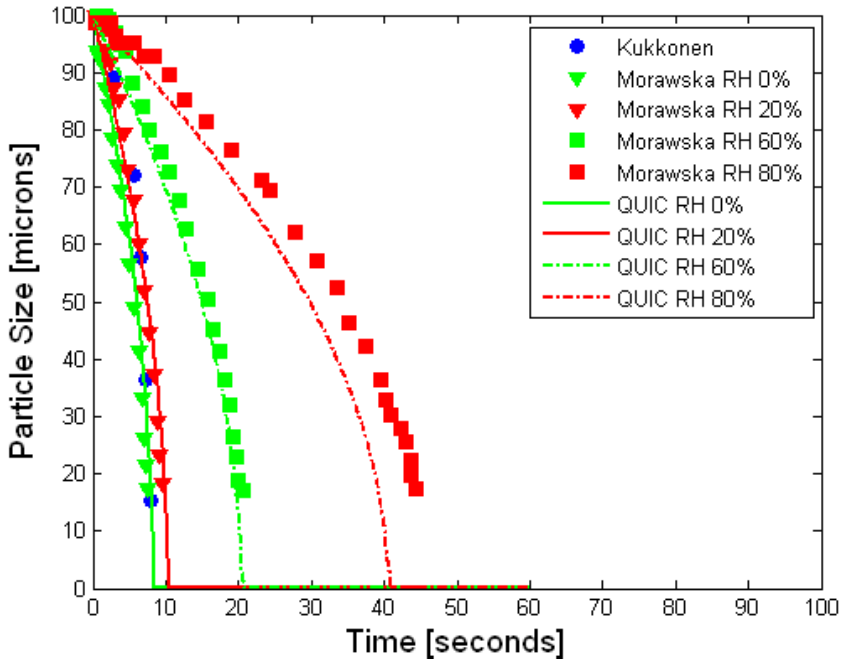

Figure 3. Comparison of QUIC droplet size results with calculations of Kukkonen et al. (1989, dry air) and Morawska (2006) for freely falling droplets.

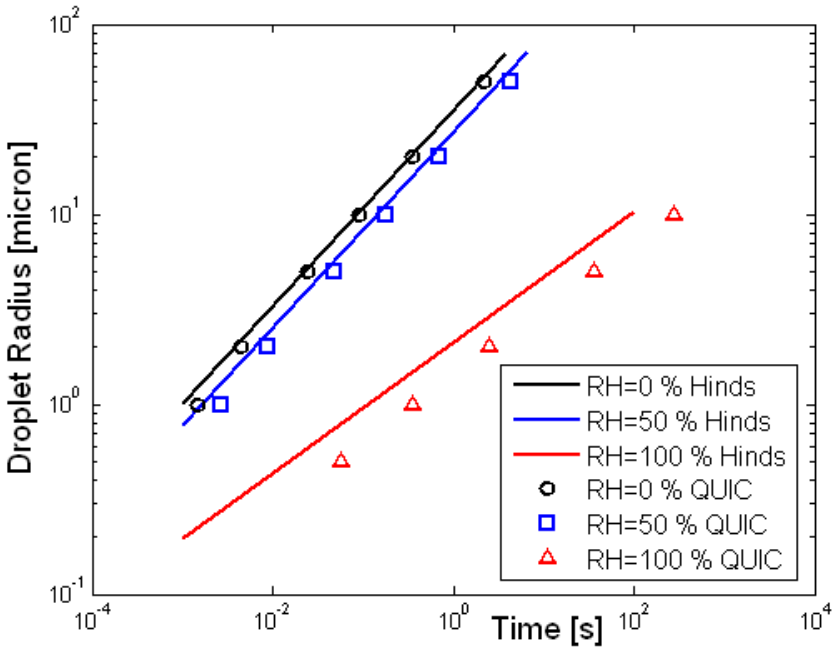

Figure 4. Comparison of drying times for freely falling pure water droplets of different sizes at temperature 20 °C: Hinds' model (lines); QUIC model (symbols).

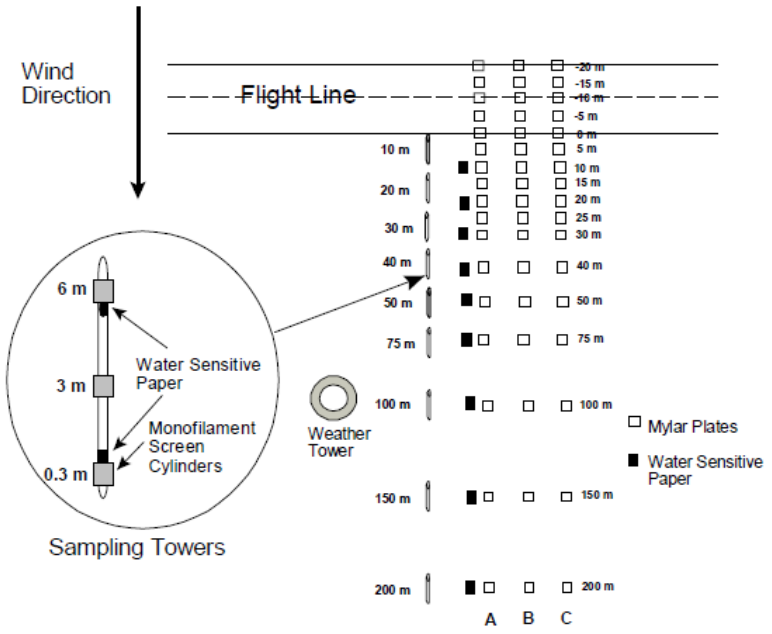

Figure 5. Field test geometry and distribution of equipment (Fritz and Hoffmann, 2007).

Rep	Time of Acquisition	Temp.at 2.5 m (°C)	Relative Humidity (%)	Wind Speed at 2.5 m (m/s)	Ri[1]
1	7:16 am	21.5	95.7	0.01	0.82
2	7:43 am	23.0	92.1	0.4	-0.77
3	8:02 am	24.2	88.7	0.9	-3.4
4	8:18 am	24.8	86.2	0.8	-717
5	8:35 am	25.8	82.7	0.9	-1.8
6	8:50 am	26.6	79.0	0.9	-22
7	7:04 pm	34.5	37.8	2.3	-0.030
8	7:20 pm	34.1	38.7	2.2	0.048
9	7:36 pm	33.5	42.1	1.9	0.081
10	7:52 pm	33.3	42.2	2.1	0.086
11	8:08 pm	32.6	44.5	2.1	0.11
12	8:24 pm	31.4	48.3	1.4	0.22

Table 1. Meteorological conditions measured and calculated during field tests (Fritz and Hoffmann 2007).

Rep	Integrated Deposition In-swath (% Applied)	Integrated Downwind Deposition 0-200 m (% Applied)
1	73	25
2	78	17
3	56	33
4	66	22
5	60	17
6	51	20
7	38	22
8	60	13
9	34	15
10	40	10
11	33	12
12	45	15

Table 2. Measured in-swath and downwind deposition (Fritz and Hoffmann 2007).

		Downwind Distance (m)									
	Rep	0-10	10-20	20-30	30-40	40-50	50-75	75-100	100-150	150-200	Total
Incremental Deposition (% of Applied)	1	14	5.7	2	0.9	0.6	1	0.2	0.2	0.1	25
	2	10	2.2	1	0.8	0.5	0.7	0.4	0.4	0.2	17
	3	20	5.5	3.2	2	0.9	0.9	0.3	0.3	0.1	33
	4	17	2.4	0.9	0.2	0.2	0.4	0.1	0.1	0.1	22
	5	13	1.8	0.8	0.3	0.3	0.2	0.1	0.2	0.1	17
	6	15	2.9	0.9	0.5	0.3	0.2	0.1	0.1	0.1	20
	7	7.3	4.5	3.3	2.3	2.4	0.8	0.7	0.5	0.5	22
	8	7.2	2.8	0.9	0.3	0.5	0.3	0.6	0.4	0.2	13
	9	8.1	3.6	1	0.4	0.5	0.4	0.6	0.4	0.4	15
	10	4.4	2.1	0.8	0.5	0.4	0.3	0.5	0.4	0.3	10
	11	5.8	2.1	0.9	0.5	0.8	0.4	0.6	0.4	0.4	12

Table 3. Downwind deposition as a function of downwind distance (Fritz and Hoffmann 2007).

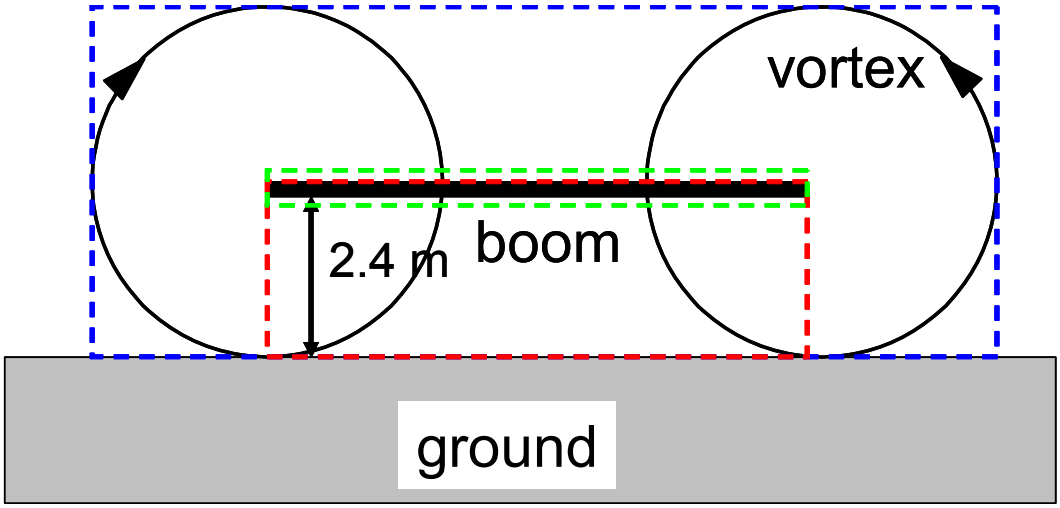

Figure 6. Geometry of sources used in QUIC simulations.

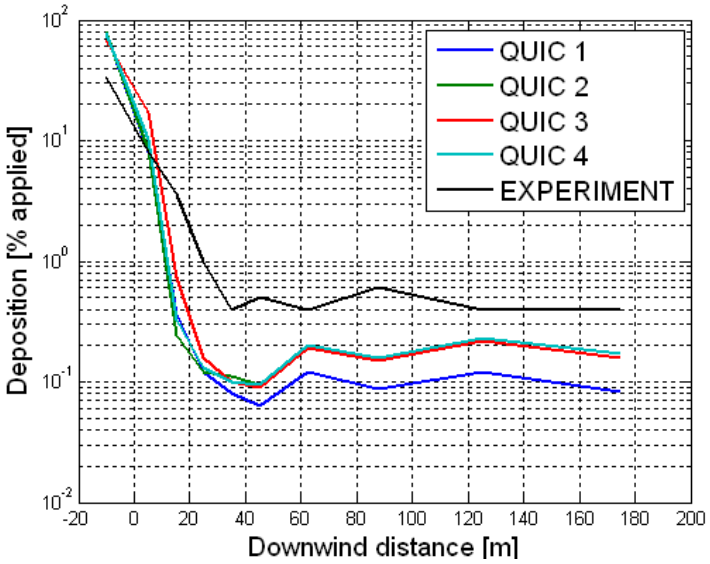

Figure 7. Comparison of experimental measurements and model-computed deposition for case 9 (1/L=0.047). Numbers in legend (QUIC 1-4) denote QUIC runs: 1-neutral stability, source depth 2.4 m; 2-stable, source depth 2.4 m; 3-stable, source depth 4.8 m and 4-stable, thin elevated source. In-swath spray region spans from -20 to 0 m.

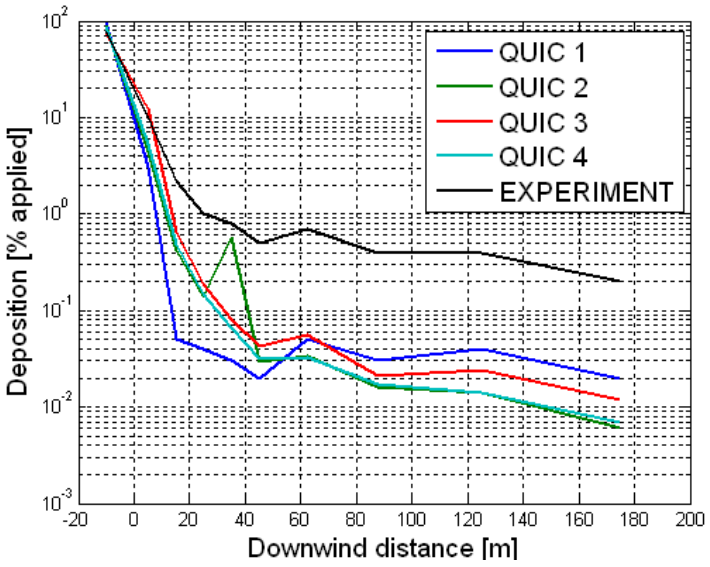

Figure 8. Comparison of experimental measurements and model-computed deposition for case 2 (1/L=-0.24). Numbers in legend (QUIC 1-4) denote QUIC runs: 1-neutral stability, source depth 2.4 m; 2-unstable, source depth 2.4 m; 3-unstable, source depth 4.8 m and 4-unstable, thin elevated source. The in-swath spray region spans from -20 to 0 m.